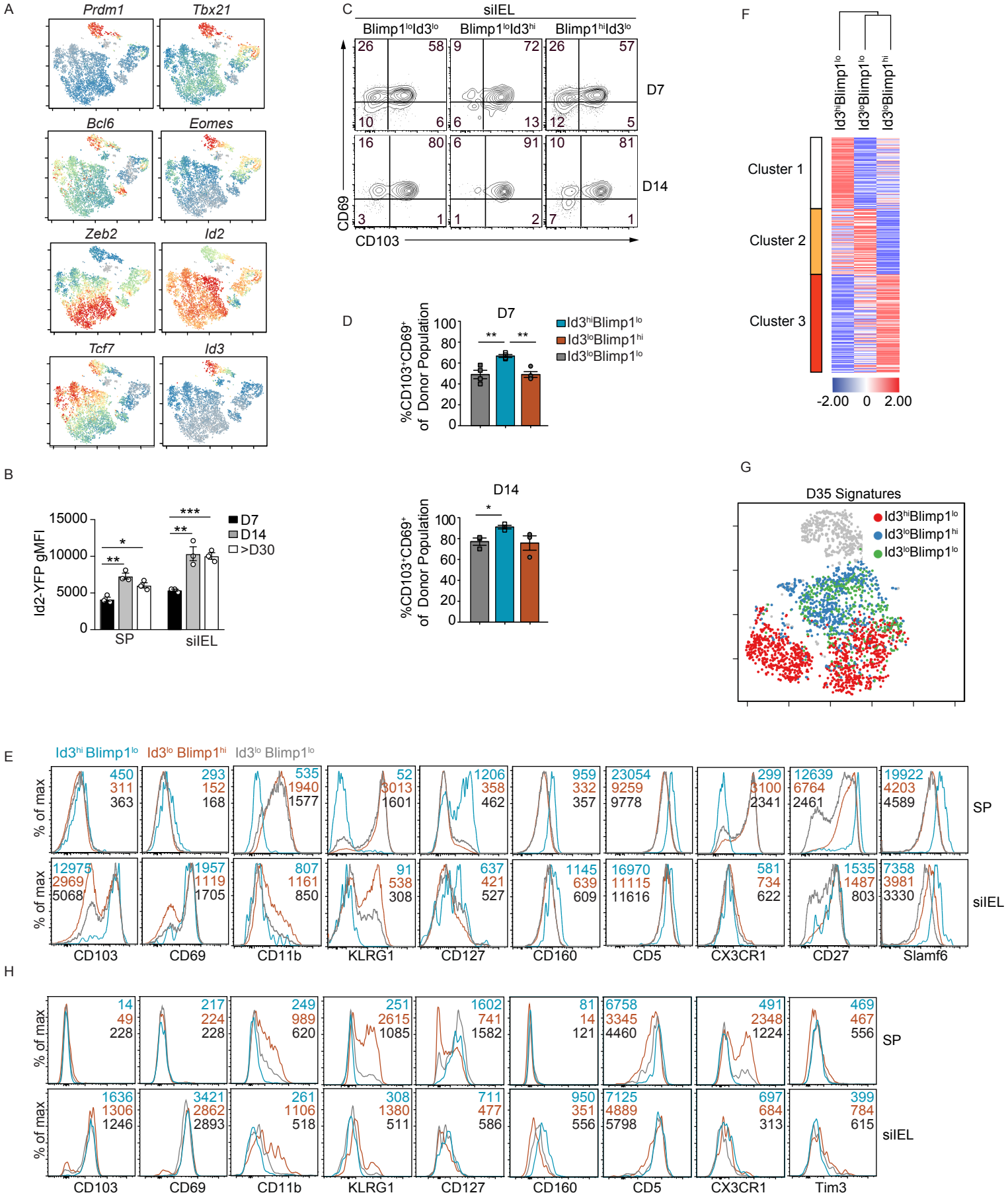
A
Prdm1
Tbx21
Bcl6
Eomes
Zeb2
Id2
Tcf7
Id3
B
Id2-YFP gMFI
15000
10000
5000
0
SP
siIEL
D7
D14
>D30
C
siIEL
Blimp1loId3lo
Blimp1loId3hi
Blimp1hiId3lo
D7
D14
CD69
CD103
D
D7
D14
%CD103+CD69+ of Donor Population
Id3hiBlimp1lo
Id3loBlimp1hi
Id3loBlimp1lo
F
Id3hiBlimp1lo
Id3loBlimp1lo
Id3loBlimp1hi
Cluster 1
Cluster 2
Cluster 3
-2.00
0
2.00
G
D35 Signatures
Id3hiBlimp1lo
Id3loBlimp1hi
Id3loBlimp1lo
E
Id3hi Blimp1lo
Id3lo Blimp1hi
Id3lo Blimp1lo
% of max
SP
siIEL
CD103
CD69
CD11b
KLRG1
CD127
CD160
CD5
CX3CR1
CD27
Slamf6
H
% of max
SP
siIEL
CD103
CD69
CD11b
KLRG1
CD127
CD160
CD5
CX3CR1
Tim3

Figure S1. Heterogeneity in anti-viral CD8$^+$ T cell populations (Related to Figures 2 and 3). (A) P14 CD8$^+$ T cells were transferred into congenically distinct hosts that were subsequently infected with LCMV i.p. Donor cells from the spleen and siIEL were sorted over the course of infection for scRNA-seq. tSNE plots of cells from the spleen over all infection timepoints shaded by intensity of relative expression of indicated transcriptional regulator. **(B)** Id2-YFP/Id3-GFP P14 CD8+ T cells were transferred into congenically distinct hosts that were infected with LCMV i.p. At indicated times of infection, Id2-YFP reporter expression was analyzed in the P14 cells isolated from the spleen and siIEL by flow cytometry and the gMFI is quantified. **(C-F)** Congenically distinct Blimp1-YFP/Id3-GFP P14 CD8$^+$ T cells were transferred to wild-type hosts that were subsequently infected with LCMV i.p. **(C)** CD103 and CD69 expression on indicated populations is shown. **(D)** Quantification of populations in C. **(E)** On day 7 of infection, Id3^{hi}Blimp1^{lo}, Id3^{lo}Blimp1^{hi}, and Id3^{lo}Blimp1^{lo} P14 CD8$^+$ T cells from spleen (SP) and siIEL were analyzed by flow cytometry. **(F)** On day 35 of infection, Id3^{hi}Blimp1^{lo}, Id3^{lo}Blimp1^{hi}, and Id3^{lo}Blimp1^{lo} P14 CD8$^+$ T cells were sorted from siIEL for RNA-sequencing. A heatmap illustrating the relative expression of genes differentially expressed among the 3 sorted populations is shown; gene clusters are ordered through K-means clustering analysis. **(G)** As in A, tSNE plots of cells from the siIEL over all timepoints shaded by intensity of indicated transcriptional signatures at day 35 following LCMV infection. **(H)** As in E, Id3^{hi}Blimp1^{lo}, Id3^{lo}Blimp1^{hi}, and Id3^{lo}Blimp1^{lo} P14 CD8$^+$ T cells from spleen (SP) and siIEL were analyzed by flow cytometry on day 25-27 of infection. Numbers in plots represent the frequency of cells in the indicated gate (C) or gMFI (E,H). All data are from one representative experiment of 2 independent experiments with n=3. Graphs show mean ± SEM; *p<0.05, **p<0.01, ***p<0.001.

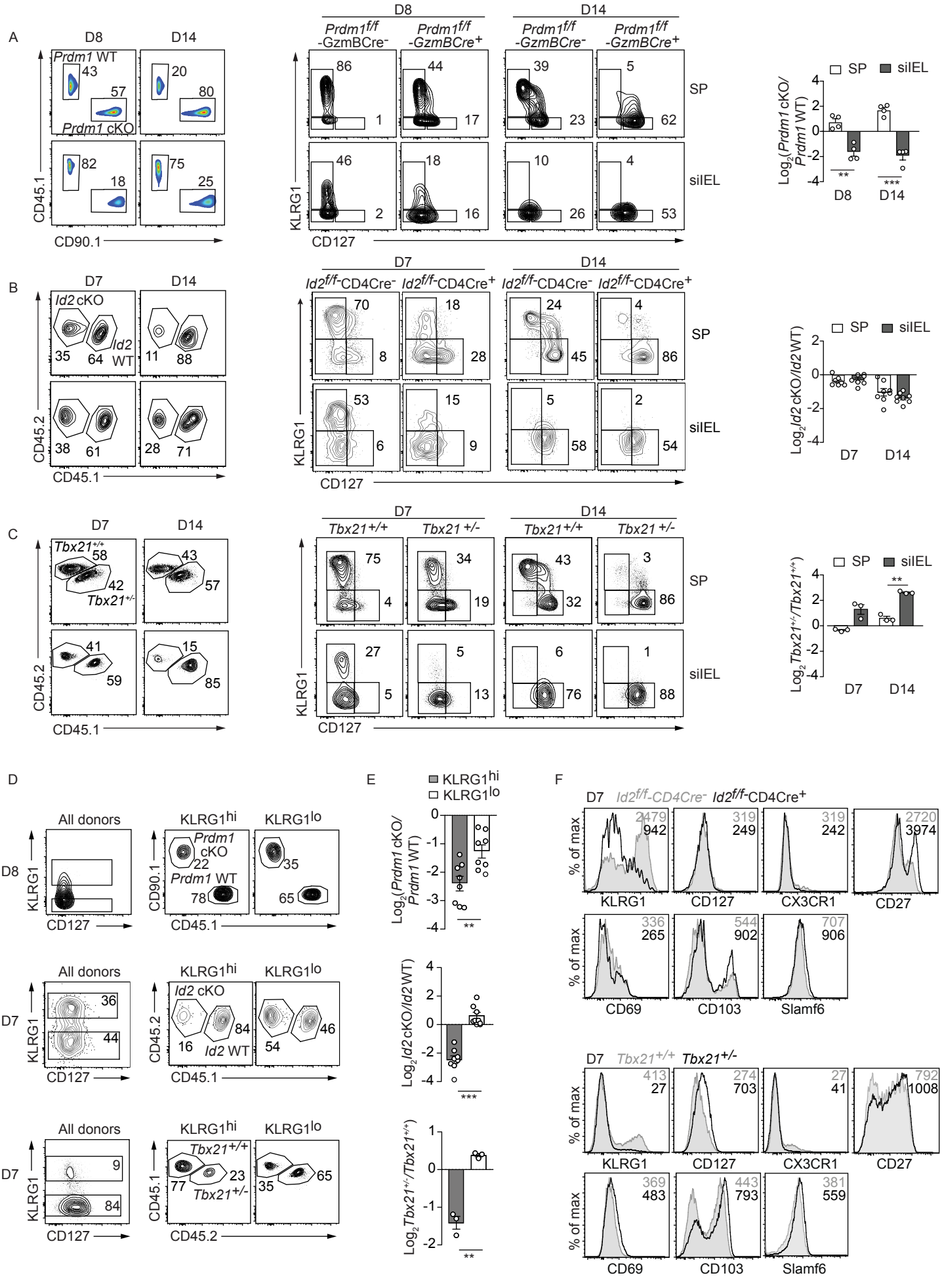
A
D8
D14
Prdm1 WT
Prdm1 cKO
CD45.1
CD90.1
Prdm1f/f -GzmBCre-
Prdm1f/f -GzmBCre+
SP
siIEL
KLRG1
CD127
Log2(Prdm1 cKO/ Prdm1 WT)
B
D7
Id2 cKO
Id2 WT
CD45.2
Id2f/f-CD4Cre-
Id2f/f-CD4Cre+
Log2(Id2 cKO/Id2 WT)
C
Tbx21+/+
Tbx21+/-
Log2(Tbx21+/-/Tbx21+/+)
D
All donors
KLRG1hi
KLRG1lo
E
F
% of max
KLRG1
CD127
CX3CR1
CD27
CD69
CD103
Slamf6

Figure S2. Pro-effector transcriptional regulators control siIEL CD8$^+$ T cell differentiation (Related to Figure 5). Mixed transfer of congenically distinct Prdm1$^{f/f}$-GzmBCre$^+$ (Prdm1 cKO) and Prdm1$^{+/+}$ (Prdm1 WT), Id2$^{f/f}$-CD4Cre$^+$ (Id2 cKO) and Id2$^{f/f}$-CD4Cre$^-$ (Id2 WT) or Tbx21$^{+/-}$ and Tbx21$^{+/+}$ P14 CD8$^+$ T cells into recipient mice that were subsequently infected with LCMV. Donor P14 cells from host spleen and siIEL were analyzed by flow cytometry at indicated times of infection. **(A-C)** Frequency of indicated donor populations among CD8$^+$ T cells and corresponding quantification is shown (left). KLRG1 and CD127 expression on indicated donor populations is represented (middle/right). **(D)** KLRG1^{hi} and KLRG1^{lo} populations of all donor P14 CD8$^+$ T cells from the siIEL (left) and the frequency of the donor cells within these populations (right) is shown. **(E)** Quantification of populations from D. **(F)** Expression of indicated molecules is compared between Id2$^{f/f}$-CD4Cre$^+$ and Id2$^{f/f}$-CD4Cre$^-$ (top) or Tbx21$^{+/-}$ and Tbx21$^{+/+}$ (bottom). Numbers in plots represent the frequency (A-D) or gMFI (F) of cells in the indicated gate. All data are from one representative experiment of 2 independent experiments with n=3-5. Graphs show mean ± SEM; **p<0.01, ***p<0.001.

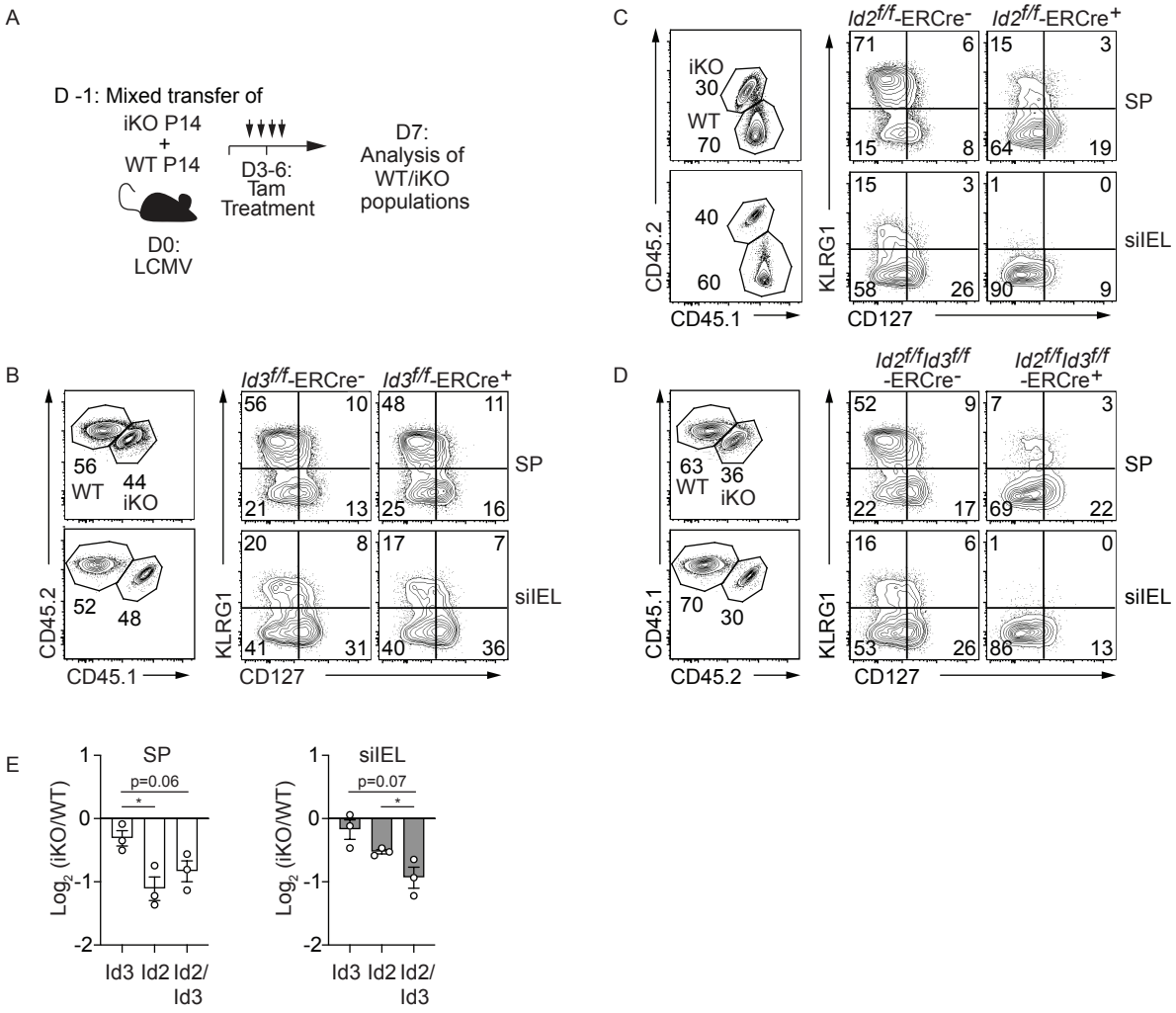

Figure S3. Id2 and Id3 mediate the formation of siIEL CD8⁺ T cell populations (Related to Figure 5). (A) Schematic of experimental set-up. A mix of congenically distinct Id2$^{f/f}$-ERCre^{+}, Id3$^{f/f}$-ERCre^{+}, or Id2$^{f/f}$Id3$^{f/f}$ -ERCre^{+} (iKO) and corresponding wild type ERCre^{-} (WT) P14 CD8^{+} T cells were transferred to recipients that were subsequently infected with LCMV i.p. On day 3 of infection, host mice were treated for 4 consecutive days with tamoxifen (Tam) to induce **(B)** Id3, **(C)** Id2 or **(D)** Id2 and Id3 deletion. Transferred P14 CD8^{+} T cells from host spleen (SP) and siIEL were analyzed by flow cytometry on day 7 of infection. Frequency of WT and iKO cells among P14 CD8^{+} T cells (left) and corresponding KLRG1 and CD127 expression (right) is represented. **(E)** Quantification of the frequency of indicated populations is displayed. Data are expressed as mean ± SEM. Numbers in plots represent frequency of cells in the indicated gate. All data are from one experiment with n=3. Graphs show mean ± SEM; *p<0.05, **p<0.01.

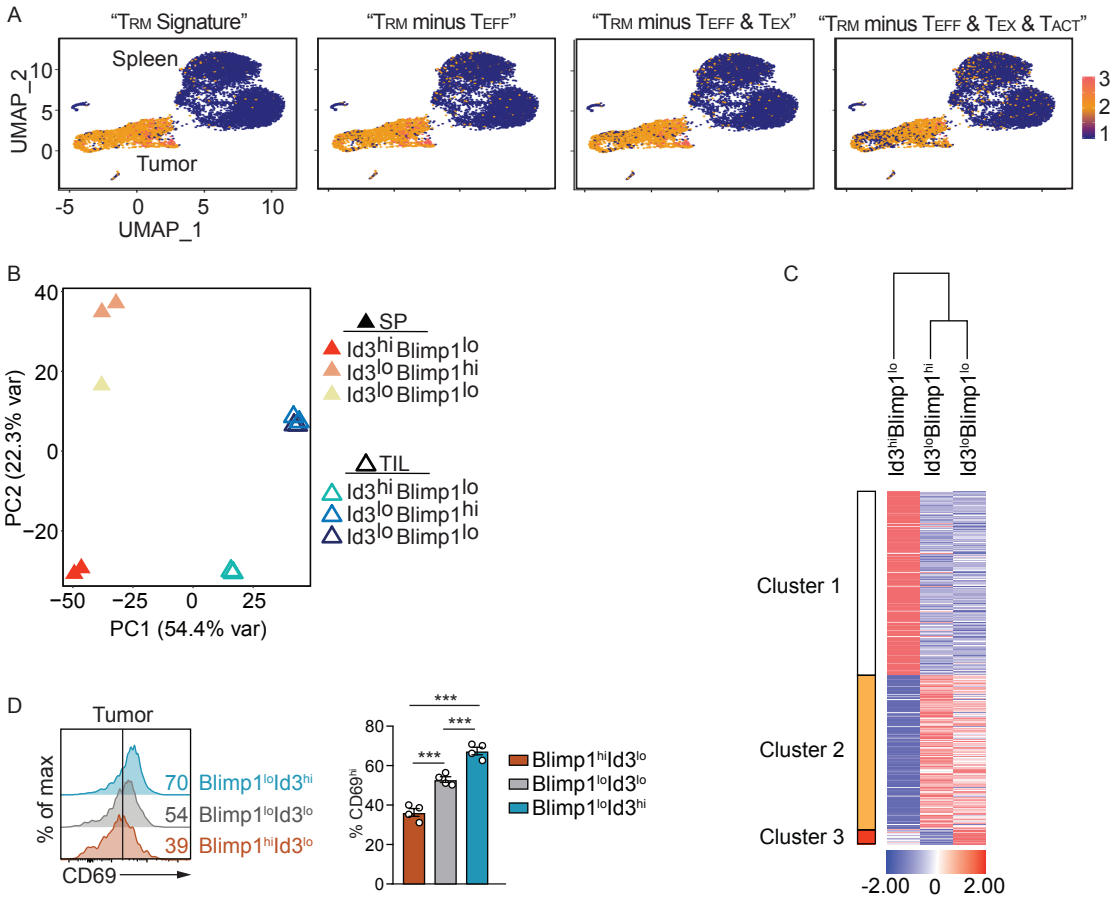

Figure S4. Heterogeneity in Trm cell-like TIL populations (Related to Figure 6). Congenically distinct WT or Id3-GFP/Blimp1-YFP P14 cells were transferred into B16-GP$_{33-41}$ tumor-bearing mice, and one-week post adoptive transfer, WT P14 CD8$^+$ T cells were sorted from spleen and tumors for scRNA-Seq analysis and Id3^{hi}Blimp1^{lo}, Id3^{lo}Blimp1^{hi}, and Id3^{lo}Blimp1^{lo} P14 CD8$^+$ T cells were sorted for bulk RNA-Seq analysis, or analyzed by flow cytometry. **(A)** UMAP plot of WT P14 cells sorted from tumor and spleen indicating relative enrichment of the core tissue-residency signature (left) and the same list with the removal of characteristic effector T cell (middle left), exhausted T cell (middle right) and activated T cell (right) associated genes. **(B)** Principal component analysis of gene expression from the sorted P14 CD8$^+$ T cells from tumors is shown. **(C)** Heatmap illustrating the relative expression of genes differentially expressed among the 3 sorted populations is shown; populations are ordered through hierarchical clustering analysis and gene clusters are ordered through K-means clustering analysis. **(D)** Donor cells from tumors were analyzed for CD69 expression. Numbers in plots represent frequency of cells in the indicated gate. All data are from one representative experiment with n=4. Graphs show mean ± SEM; ***p<0.005.

Supplemental Table 1. Effector Gene Signature (related to Figure 1)

1700017B05Rik	Cd86	Ezh2	Itgb1	Prr13	Top2a
2010002N04Rik	Cdc20b	F630043A04Rik	Jup	Prr5l	Tpx2
2010012O05Rik	Cdc25b	Fam129a	Kif11	Prune	Trdn
2610029I01Rik	Cdk1	Fancm	Kif15	Ptms	Trio
2810417H13Rik	Cdk2	Fhl2	Kif22	Pus10	Tspan2
2810417H13Rik	Cenpa	Fkbp5	Kif23	Pycard	Tspan32
3110052M02Rik	Cenpe	Gabarapl1	Klra10	Rab11fip4	Ubash3b
4930447A16Rik	Cenpk	Galnt3	Klra3	Racgap1	Unc119
4930515G01Rik	Cep55	Gem	Klra6	Rap1gap2	Usp3
4930547N16Rik	Cep76	Glcci1	Klra8	Rbms1	Usp46
6330403K07Rik	Cercam	Gm10286	Klre1	Reep5	Whsc1
A630007B06Rik	Chd7	Gm10785	Klrg1	Rhoq	Xlr
Adam17	Chn2	Gm10786	Kntc1	Rnf19a	Xpnpep1
Ahnak	Chsy1	Gm11277	Lag3	Rnf216	Zeb2
AI597468	Cited2	Gm14005	Lamc1	Rnpep	Zfand5
Ak3	Cldnd2	Gm4884	Lass6	Rora	Zfp40
Alcam	Cmklr1	Gm8615	Lgals1	Rrm2	Zfp874b
Anln	Cmpk1	Gna15	Lgals3	S100a4	
Anxa4	Cry1	Gpx8	Lmnb1	S1pr5	
Apaf1	Crybg3	Grxcr1	LOC100503984	Scd2	
Apobec2	Csda	Gsn	Lxn	Serinc5	
Arhgap11a	Csnk1e	Gzma	Manba	Serpinb6b	
Arhgap19	Ctnnbip1	Gzmb	Mki67	Shcbp1	
Arhgef12	Ctsc	Gzmk	Msc	Slc25a20	
Arntl	Cx3cr1	Havcr2	Mxi1	Slc25a33	
Art2a-ps	Cyp3a16	Hbb-b2	Ncapg	Slc25a45	
As3mt	D330041H03Rik	Hiatl1	Ndnl2	Slc4a7	
Asna1	Dapk2	Hist1h1b	Nebl	Snx10	
Atoh1	Dclk2	Hist1h2ab	Nipal3	Snx5	
Atp2a3	Ddx19b	Hist1h2ak	Nqo2	Sord	
Atp6v1d	Ddx28	Hist1h2bf	Nrp1	Sp140	
AU022870	Dennd5a	Hist1h2bj	Olfr598	Spag1	
BC013712	Depdc1a	Hist1h2bk	Olfr766	Spag5	
Bhlhe40	Depdc1b	Hist1h2bm	Osbpl3	Spast	
Bub1	Dhx40	Hist1h2bn	Osbpl8	Spc25	
Bub1b	Dlgap5	Hmgb2	Palm	Spn	
C330027C09Rik	Dnajc1	I830127L07Rik	Pdcd1	Sptlc2	
Car5b	Dock5	Icos	Pgm2l1	Stmn1	
Carhsp1	Dtl	Idh2	Pld4	Stx11	
Casc5	Dync1li2	Igf2bp3	Plek	Sun1	
Casp3	E2f2	Il18rap	Plekhf1	Suox	
Casp7	E2f8	Inpp4a	Plekho1	Swap70	
Ccna2	Efhd2	Irf4	Pmaip1	Tbcc	
Ccnb1	Emp1	Itga2	Pola1	Tbkbp1	
Ccnb2	Ern1	Itga4	Prc1	Timp2	
Ccne2	Esm1	Itgam	Prdm1	Tmem165	
Cd68	Etfb	Itgax	Prdx4	Tmf1	

Supplemental Table 2. Memory Gene Signature (related to Figure 1)

Gene_Symbol							
0610037L13Rik	B3galt6	D17H6S56E-5	Fam116b	Gtpbp4	Mat2a	Nsg2	Rabggtb
1600012F09Rik	Bach2	D630037F22Rik	Fam122b	H2-Ob	Mboat1	Nt5e	Rapgef6
1700021A07Rik	Bat1a	Dapl1	Fam125b	Haus5	Mcoln2	Oasl2	Rcl1
1700021C14Rik	Bbs2	Dars	Fam134b	Heatr1	Mdn1	Olfr316	Rgs10
2410002F23Rik	BC005685	Dctd	Fam169b	Heatr5a	Mettl1	P2ry10	Rnaseh2a
2410066E13Rik	BC016423	Ddx18	Fam46a	Hectd2	Mgrn1	Pa2g4	Rnf122
2610019F03Rik	BC048403	Ddx51	Fam46c	Herpud1	Mid1	Paics	Rnf130
2610030H06Rik	BC049349	Ddx56	Farsb	Hexa	Mif	Pam	Rnf141
4732471D19Rik	BC057079	Ddx60	Fastkd2	Hipk2	Mipep	Parp12	Rnf144a
4930420K17Rik	Bckdhb	Dennd2d	Fcgr2b	Hook1	Mir29c	Parp8	Rny1
4930522L14Rik	Bcl2	Dennd4a	Fchsd2	Hs3st3b1	Mir342	Pde2a	Rny3
4933439F18Rik	Bcl7a	Dguok	Fntb	Hsd17b11	Mki67ip	Pdk2	Rpl10
5830405N20Rik	Bmpr1a	Dhdds	Foxp1	Hsd17b12	Mmab	Pdlim1	Rpl10a
6330409N04Rik	Bnip3	Dirc2	Fpgs	Hsp90aa1	Mmachc	Pebp1	Rpl11
6530401N04Rik	Brix1	Dkc1	Fpgt	Hsp90ab1	Mov10	Pex3	Rpl12
A2ld1	Btbd11	Dkkl1	Gaa	Hspe1	Mrpl23	Pgm3	Rpl13
A630038E17Rik	Btbd19	Dmrta1	Gapdhs	Hus1	Mrpl35	Pilrb2	Rpl15
AB041803	Btla	Dnajb2	Gart	Hvcn1	Mrpl38	Pisd-ps1	Rpl21
AB124611	C1qbp	Dock6	Gas5	Ier3	Mrpl52	Pkp4	Rpl21-ps10
Abca1	C230055K05Rik	Dock9	Gas7	Ifi30	Mrps18b	Plekha1	Rpl23
Abcc1	Cad	Dph5	Gbe1	Ifrd2	Ms4a4a	Plrg1	Rpl23a
Abce1	Cbx7	Dse	Gm10345	Ift172	Ms4a4c	Pltp	Rpl27
Abhd11	Ccdc101	Dtx1	Gm11968	Ikbkb	Mtg1	Polr1a	Rpl27a
Abhd14b	Ccnd2	Dtx4	Gm12191	Il10rb	Mthfd1	Polr1b	Rpl29
Abhd6	Ccr7	Dus4l	Gm13139	Il2ra	Mtx3	Polr2e	Rpl3
Acsl1	Cd2ap	Dynlt3	Gm14326	Il2rb	Mybbp1a	Polr3e	Rpl30
Acvr1b	Cd44	Dzip1	Gm14391	Il4ra	Myc	Pomt1	Rpl31
Acvr2a	Cd55	E430029J22Rik	Gm14403	Il6ra	Myo3b	Pou6f1	Rpl32
AI480653	Cd69	Echdc1	Gm14420	Il6st	Naa10	Ppie	Rpl35
Aldh6a1	Cd7	Edaradd	Gm16489	Il7r	Naa25	Ppih	Rpl36
Aldoa	Cd72	Eef1e1	Gm4979	Impdh2	Naip5	Ppp1r14b	Rpl36a
Alg1	Cd93	Eef2k	Gm4983	Inadl	Nat10	Pprc1	Rpl38
Alg8	Cdh1	Efha2	Gm5244	Inpp4b	ND3	Prdx6	Rpl39
Ampd3	Cdk4	Ehd3	Gm5921	Insr	Ndufa4	Prmt7	Rpl41
Apex1	Celsr1	Eif4a2	Gm9104	Ipo4	Ndufa5	Pros1	Rpl8
Apol7b	Cenpt	Elovl5	Gm9457	Jmjd8	Ndufaf4	Prrg1	Rpl9
Apol7e	Chic1	Emb	Gng5	Kbtbd11	Nek1	Prrg4	Rplp1
Aqp9	Cisd1	Enpp4	Gnl3	Kcnj8	Neurl3	Prss12	Rpp38
Arhgap39	Cnbp	Enpp5	Gpatch4	Lipo1	Nle1	Psme1	Rpp40
Arhgap5	Cnr2	Entpd5	Gpr114	Lmbr1	Nme1	Psmg1	Rps10
Arrb1	Cnrip1	Entpd6	Gpr155	LOC641050	Nme2	Ptges3	Rps12
Ass1	Coro2a	Eral1	Gpr183	Lpar5	Nol6	Ptma	Rps14
Atg14	Crim1	Ergic1	Gpr97	Ltb	Nop10	Pus7	Rps15
Atn1	Crtam	Erich1	Gpx1	Ly6a	Nop16	Pwp2	Rps15a
Atp6v0d2	Cst7	Evl	Gramd4	Ly6e	Nop56	Qser1	Rps16
Atp8a2	Ctdsp2	Exosc1	Grwd1	Lyplal1	Nop58	Qtrtd1	Rps2
Atpbd4	Ctss	Faah	Gstk1	Map4k3	Nr1d1	Rab37	Rps23
B230307C23Rik	Cxcr4	Fam101b	Gsto1	Mapk11	Nr1d2	Rab6b	Rps24
B230315N10Rik	D130062J21Rik	Fam102a	Gstp1	Mars2	Nr2c1	Rabac1	Rps26

Rps27	Snord47	Trmt61a	Zscan12
Rps28	Snord49b	Trove2	
Rps3	Snord53	Trp53	
Rps5	Snord57	Tsga10ip	
Rps8	Snord8	Tspan13	
Rps9	Snord95	Tspan31	
Rpsa	Snrpg	Tsr1	
Rrp15	Snx16	Tsr2	
Rrp1b	Socs3	Ttc27	
Rtp4	Spef2	Ttc28	
Rundc3b	Spint2	Tuba1b	
Samd3	Srm	Tuba1c	
Satb1	Ssbp2	Tuba4a	
Scamp4	Ssh2	Tubb5	
Scarna13	Suclg2	Uba52	
Sell	Surf2	Ube2cbp	
Serpina3f	Taf1d	Unc5a	
Sesn3	Taf4b	Urb1	
Sfxn1	Tasp1	Ust	
Sh3bp5	Tcf7	Utp15	
Sigmar1	Tcfap4	Utp20	
Sil1	Tdrd7	Uxt	
Sit1	Tfrc	Vars	
Slc11a2	Tgtp1	Vipr1	
Slc12a7	Thada	Vkorc1	
Slc14a1	Thoc1	Vmn2r29	
Slc19a1	Thra	Vmn2r86	
Slc26a11	Timm10	Vwa5a	
Slc7a1	Timm8a1	Wbscr27	
Slc7a5	Tmem38b	Wdr12	
Slfn1	Tmem48	Wdr18	
Slfn5	Tmem63a	Wdr36	
Smyd2	Tmx2	Wdr46	
Smyd3	Tnf	Wdr49	
Smyd5	Tnfrsf18	Wwp1	
Snhg1	Tnfrsf22	Xcl1	
Snora21	Tnfrsf26	Xrcc5	
Snora23	Tnfsf10	Yars2	
Snora3	Tnfsf8	Yes1	
Snora44	Tpi1	Zbtb20	
Snora52	Tpt1	Zcwpw1	
Snora61	Traf1	Zdhhc23	
Snora62	Treml2	Zeb1	
Snora69	Trim12a	Zfp110	
Snora7a	Trim30d	Zfp238	
Snord104	Trio	Zfp280d	
Snord1c	Trmt1	Zfp781	
Snord32a	Trmt112	Zhx2	
Snord35a	Trmt5	Zmat1	